This is the accepted manuscript (postprint) of the following article:
S. Rastegari, E. Salahinejad, *Morphological Optimization of Chemical-Conversion Sodium Titanate and Chitosan/Glass Nanocomposite Dip Coatings Deposited on a Titanium Alloy*, Metals and Materials International, 26 (2020) 188-195.
https://doi.org/10.1007/s12540-019-00315-1

Morphological optimization of chemical-conversion sodium titanate and chitosan/glass nanocomposite dip coatings deposited on a titanium alloy

S. Rastegari, E. Salahinejad*

Faculty of Materials Science and Engineering, K. N. Toosi University of Technology, Tehran, Iran

Abstract

In this paper, the effect of some parameters of a two-step surface-modification process, consisting of alkaline treatment followed by chitosan/bioactive glass nanocomposite coating, on the surface morphology of Ti-6Al-4V alloy is investigated. According to the results, the heat treatment of the alkaline-treated sample is critical to obtain a crack-free structure. It was also found that the deposition of three composite layers with the immersion time of 3 min for each layer is optimal to develop a desirable distribution of the composite nanoparticles on the surface. In other words, a coordinated optimization approach of composite-coating variables is required to control the morphology of the deposits.

Keywords: Titanium alloys; Alkaline treatment; Nanocomposite coatings

* Corresponding Author: Email Address: <salahinejad@kntu.ac.ir>

This is the accepted manuscript (postprint) of the following article:
S. Rastegari, E. Salahinejad, *Morphological Optimization of Chemical-Conversion Sodium Titanate and Chitosan/Glass Nanocomposite Dip Coatings Deposited on a Titanium Alloy*, Metals and Materials International, 26 (2020) 188-195.
https://doi.org/10.1007/s12540-019-00315-1

1. Introduction

Commercially pure titanium and titanium-based alloys are extensively used to fabricate orthopedic and dental implants due to their suitable mechanical properties, chemical stability and biocompatibility [1, 2]. However, the long-term performance of these alloys in the body demands more improvements in bioactivity [3-8] and biocompatibility [9, 10]. To address these drawbacks, a number of surface-modification techniques have been reported in the literature, including conversion and composite coatings [11].

Among different conversion coatings applied on medical-grade titanium alloys, NaOH alkaline treatment yields significant apatite-formation ability and bioactivity [12-14]. Nevertheless, this treatment imposes unsuitable contributions to the growth and proliferation of cells due to the local increase of pH [15]. To solve the problem, the deposition of additional coating layers on the alkaline-treated surface, including hydroxyapatite/chitosan [16] and $2SiO_2$-CaO-MgO glass/chitosan [17] composite coatings has been shown to be effective. Evidently, the resulted biological properties of this type of double-layered coatings (particularly bioactivity and biocompatibility) are dependent on final surface characteristics (including morphology) which are determined by coating parameters. To our knowledge, there are no integrated reports in the literature on the effect of the heat treatment of the alkaline-treated surface, the number of the deposited composite layers and the dipping immersion time of each composite layer on the morphology of this type of surfaces (alkaline + composite coatings), which is the subject of this paper.

2. Experimental procedures

2.1. Synthesis of glass nanoparticles

This is the accepted manuscript (postprint) of the following article:
S. Rastegari, E. Salahinejad, *Morphological Optimization of Chemical-Conversion Sodium Titanate and Chitosan/Glass Nanocomposite Dip Coatings Deposited on a Titanium Alloy*, Metals and Materials International, 26 (2020) 188-195.
https://doi.org/10.1007/s12540-019-00315-1

Coprecipitation followed by calcination was used to synthesize $2SiO_2$-CaO-MgO glass powders, according to Refs. [18-20]. Calcium chloride ($CaCl_2$, Merck, > 98%), magnesium chloride ($MgCl_2$, Merck, > 98%) and silicon tetrachloride ($SiCl_4$, Merck, > 99%) were employed as precursors for Ca, Mg and Si species, respectively. Also, dry ethanol (C_2H_5OH, Merck, > 99%) and aqueous ammonia solution (NH_4OH, Merck, 25%) were utilized as the solvent and precipitating agent, respectively. An equimolar amounts of $CaCl_2$ and $MgCl_2$ were first dissolved in ethanol. Afterwards, a double-molar amount of $SiCl_4$ was added to this solution embedded in an ice-water bath, giving the cationic stoichiometry of diopside ($CaMgSi_2O_6$). The ammonia solution was then dropwise added until a pH value of about 10. Finally, the obtained participates were dried at 120 °C for 6 h and calcined at 500 °C for 2 h.

2.2. Preparation of the composite sol

Chitosan (Sigma Aldrich, deacetylation degree: 84.2%, molecular weight: 140469.4 g/mol) was dissolved in 2% acetic acid (Mojallali, >99.9%) at the concentration of 1 gr/L. Afterwards, 1 gr of the calcined ceramic powder was added to the solution, giving a weight ratio of 50% ceramic with respect to chitosan. The mixture was stirred and then processed by a probe ultrasonicator (Qsonica, Q125) for 1 h in order to achieve a well-dispersed stable sol.

2.3. Treatments of the Ti substrate

Medical-grade Ti-6Al-4V plates of 0.1×2×2 cm^3 in size were mirror-like polished and sonicated in ethanol, acetone and distilled water baths. Three coating processes were followed on the processed substrates, including (i) alkaline treatment, (ii) composite coating, and (iii) alkaline treatment followed by composite coating. For the alkaline treatment, the

This is the accepted manuscript (postprint) of the following article:
S. Rastegari, E. Salahinejad, *Morphological Optimization of Chemical-Conversion Sodium Titanate and Chitosan/Glass Nanocomposite Dip Coatings Deposited on a Titanium Alloy*, Metals and Materials International, 26 (2020) 188-195.
https://doi.org/10.1007/s12540-019-00315-1

substrates were immersed in a 5 molar NaOH (Merck, >97%) solution at 60 °C for 24 h, followed by washing with distilled water. The samples were dried at either room temperature or 60 °C for 24 h. For the deposition of composite coatings, both alkaline-treated and non-treated specimens were once or three times dipped into the prepared composite sol with the dipping and withdrawal rates of 30 mm/s and the variable immersion durations of 0.5, 3 and 5 min. Each layer of the coating was dried at 40 °C for 24 h before applying the next layer.

2.4. Structural characterization

The silicate powder calcined at 500 °C was characterized by X-ray diffraction (XRD, PANalyticial, X'Pert Pro MPD, Cu-K_α) and Fourier transform infrared spectroscopy (FTIR, Avaspec 2048 TEC). The FTIR analysis was also used on the composite powder obtained by drying of the composite sol at 130 °C. The surface morphology and cross section of the different samples were analyzed by field-emission scanning electron microscopy (FESEM, MIRA3TESCAN-XMU).

3. Results and discussion

3.1. Characterization of the powders

The XRD spectrum of the synthesized silicate powder after calcination at 500 °C is presented in Fig. 1(a), showing no crystalline phases in the sample and confirming the full amorphicity of the synthesized glass. It is noticeable that the coprecipitation product before calcination contains a considerable amount of NH_4Cl and $NH_4(Mg(H_2O)_6)Cl_3$ [21]. It suggests the evaporation of volatile species during calcination, leaving an amorphous structure at 500 °C. Also, the calcination of the same product at 700 °C results in single-

This is the accepted manuscript (postprint) of the following article:
S. Rastegari, E. Salahinejad, *Morphological Optimization of Chemical-Conversion Sodium Titanate and Chitosan/Glass Nanocomposite Dip Coatings Deposited on a Titanium Alloy*, Metals and Materials International, 26 (2020) 188-195.
https://doi.org/10.1007/s12540-019-00315-1

phase crystalline diopside [22], inferring the equality of the loaded and obtained stoichiometries of the process.

Fig. 1(b) depicts the FTIR spectra of the glass and composite powders. The characteristic peaks of the FTIR spectra for the synthesized ceramic sample are as follows: non-bridging vibrating O-Mg-O bonds at 470 and 510 cm^{-1}, non-bridging vibrating Ca-O-Ca bonds at 418 cm^{-1}, Si-O bending mode at 670 cm^{-1}, Si-O stretching mode at 780 and 860 cm^{-1}, and Si-O-Si symmetric stretching mode at 1090 cm^{-1}, in good agreement with Refs. [21, 22] published on diopside. For the composite sample, as well as the vibrations related to the ceramic component, characteristic peaks are as follows: stretching amine groups (N-H and O-H bonds) at 3400- 3500 cm^{-1} [23-25], the stretching C-H bond at 2870-2900 cm^{-1} [23, 25], the N-H stretching bond in amide I group at 1550 cm^{-1}, the C=O stretching bond in amide group at 1650- 1700 cm^{-1}, the vibrating bond of C-H in CH_2 at 1420 cm^{-1} [23] and the C-O vibrating bond at 1000- 1100 cm^{-1} [26, 27]. This spectroscopic analysis indicates the presence of both chitosan and glass in the composite powder and proves that no side-products are formed during the preparation of the composite sol.

3.2. Morphological characterization of the coated substrates

The FESEM micrographs of the surfaces after depositing the composite coatings with the different parameters are depicted in Fig. 2. The sample covered with the mono-layered coating dipped in the composite sol for 30 sec (Fig. 2(a)) shows a low density of the glass nanoparticles of about 50 nm in diameter. In other words, a small area of the surface is covered by the nanoparticles, whereas this species is beneficial for hydrophilicity, bioactivity and biocompatibility [17, 28-31]. Additionally, in comparison to other biocoatings reported in

This is the accepted manuscript (postprint) of the following article:
S. Rastegari, E. Salahinejad, *Morphological Optimization of Chemical-Conversion Sodium Titanate and Chitosan/Glass Nanocomposite Dip Coatings Deposited on a Titanium Alloy*, Metals and Materials International, 26 (2020) 188-195.
https://doi.org/10.1007/s12540-019-00315-1

the literature, optimized samples have shown a higher population of bioactive glass and apatite nanoparticles in feature [32, 33]. Thus, keeping the weight ratio of chitosan to glass at 1:1, in order to benefit from the characteristics of the glass nanoparticles more effectively via increasing their density in the surface, two approaches were employed as follows:

(1) The increase in the dipping immersion time: Although the increase of the immersion time from 30 sec to 5 min effectively enhances the surface population of the nanoparticles (Fig. 2(b)), some areas unsuitably present a level of inhomogeneity in terms of polymer and nanoparticles agglomeration as evident in Figs. 2(c) and 2(d), respectively.

(2) The increase in the number of the deposited layers: In order to address the nanoparticle density and coating homogeneity simultaneously, three layers of the composite coating were deposited albeit with the immersion time of 3 min for each one. According to Figs. 2(e) and 2(f), the triple-layered coating represents a sound feature with respect to both two aforementioned concerns. It is worth mentioning that this morphological feature is similar to the optimized morphologies of the literature [32, 34, 35]. Thus, these coating parameters, i.e. the immersion time of 3 min with the three layers, were used hereafter. According to Fig. 3(a), this triple-layered coating has a relatively-uniform thickness of about 350 nm with no discontinuity at the coating/substrate interface.

Fig. 4 represents the FESEM micrograph of the alkaline-treated surfaces. Based on Figs. 4(a) and 4(b), the alkaline-treated surface after drying at room temperature contains some micron-sized cracks. In order to eliminate the cracks, the samples were heated at 60 °C for another 24 hours. The heating process results in the elimination of cracks, giving a homogeneous surface (Figs. 4(c) and 4(d)) and regarded as the optimal condition. The obtained morphology is described as a feather-like layer with the thickness of 500 nm (Fig.

This is the accepted manuscript (postprint) of the following article:
S. Rastegari, E. Salahinejad, *Morphological Optimization of Chemical-Conversion Sodium Titanate and Chitosan/Glass Nanocomposite Dip Coatings Deposited on a Titanium Alloy*, Metals and Materials International, 26 (2020) 188-195.
https://doi.org/10.1007/s12540-019-00315-1

3(b)) which is mostly composed of sodium titanate [36, 37]. The formed blades are evidently interconnected with a mean thickness of 70 nm, making a porous network of almost 200 nm in hollow size. The existence of cracks in the alkaline-treated surface can be explained as below. It is well established [38] that upon soaking the Ti alloy in the NaOH aqueous solution, hydroxyl groups react to the TiO_2 layer formed on the surface of Ti alloys under exposure to air:

$$TiO_2 + NaOH = HTiO_3^- + Na^+ \quad (1)$$

The simultaneous reaction of hydration also occurs:

$$Ti + 3OH^- = Ti(OH)_3^+ + 4e^- \quad (2)$$

$$Ti(OH)_3^+ + e^- = TiO_2.H_2O + 1/2H_2 \quad (3)$$

$$Ti(OH)_3^+ + OH^- = Ti(OH)_4 \quad (4)$$

The reactions imply that the alkaline treatment forms a hydrogel alkaline titanate layer on the surface. Finally, the following heat treatment process dehydrates and densifies the hydrogel layer, establishing a stable amorphous or crystalline alkaline titanate layer, which is a bioactive material [6, 39-42]. On the contrary, in case of natural drying at room temperature, as seen in Figs. 4(a) and 4(b), cracking occurs in the network due to the continued presence of the gel phase and thereby the creation of internal stresses on the dried layers.

Fig. 5 indicates the FESEM micrographs of the surfaces after the optimal alkaline treatment process followed by composite coating at the different conditions. Typically, the alkaline-treated surface after depositing one layer of the coating with the immersion time of 5 min presents a heterogeneous and agglomerated distribution of the nanoparticles (Figs. 5(a) and 5(b)). However, the deposition of the triple-layer composite coating with the immersion time of 3 min, in good agreement with Figs. 2(e) and 2(f), demonstrates a more uniform

This is the accepted manuscript (postprint) of the following article:
S. Rastegari, E. Salahinejad, *Morphological Optimization of Chemical-Conversion Sodium Titanate and Chitosan/Glass Nanocomposite Dip Coatings Deposited on a Titanium Alloy*, Metals and Materials International, 26 (2020) 188-195.
https://doi.org/10.1007/s12540-019-00315-1

distribution of the nanoparticles on the blades of the feather-like alkaline layer, as indicated in Figs. 5(c) and 5(d). The similar cross-sectional features before and after depositing the composite coating on the alkaline-treated surfaces, i.e. Figs. 3(b) and 3(c), is due to the incorporation of the composite materials into the porous network of the alkaline layer, which does not allow the composite layer in the cross-sectional view of this sample to be visible. This is in good agreement with the similarity of the top-view micrographs of the same surfaces, i.e. Figs. 4 and 5.

4. Conclusions

In order to obtain a desirable morphological feature, the affecting parameters of two surface modification methods, NaOH alkaline treatment and chitosan/glass nanocomposite coating, on a medial-grade Ti-6Al-4V alloy were optimized. According to the results, the alkaline treatment should be followed by an appropriate heat treatment process to ensure the development of a crack-free feature. Also, the suitable apparent population and uniform distribution of the glass nanoparticles in the deposited coatings was controlled by a set of the dipping immersion time and the number of the deposited layers, where the optimized values were 3 min and 3 layers, respectively, in this work.

References

1 C. Elias, J. Lima, R. Valiev and M. Meyers, *Jom* **60**, 46-49 (2008).
2 K. Wang, *Materials Science and Engineering: A* **213**, 134-137 (1996).
3 M. Geetha, A. Singh, R. Asokamani and A. Gogia, *Progress in Materials Science* **54**, 397-425 (2009).
4 Y. Oshida, *Bioscience and bioengineering of titanium materials*, Elsevier(2010).
5 M. Khan, R. L. Williams and D. F. Williams, *Biomaterials* **20**, 631-637 (1999).

This is the accepted manuscript (postprint) of the following article:
S. Rastegari, E. Salahinejad, *Morphological Optimization of Chemical-Conversion Sodium Titanate and Chitosan/Glass Nanocomposite Dip Coatings Deposited on a Titanium Alloy*, Metals and Materials International, 26 (2020) 188-195.
https://doi.org/10.1007/s12540-019-00315-1

6 S. Nishiguchi, H. Kato, H. Fujita, M. Oka, H.-M. Kim, T. Kokubo and T. Nakamura, *Biomaterials* **22**, 2525-2533 (2001).
7 L. L. Hench and J. M. Polak, *Science* **295**, 1014-1017 (2002).
8 T. Albrektsson and M. Jacobsson, *Journal of prosthetic dentistry* **57**, 597-607 (1987).
9 K. Ren, A. Dusad, Y. Zhang and D. Wang, *Acta Pharmaceutica Sinica B* **3**, 76-85 (2013).
10 R. Singh and N. B. Dahotre, *Journal of Materials Science: Materials in Medicine* **18**, 725-751 (2007).
11 D. M. Brunette, P. Tengvall, M. Textor and P. Thomsen, *Titanium in medicine: material science, surface science, engineering, biological responses and medical applications*, Springer Science & Business Media(2012).
12 H.-M. Kim, F. MIYAJI, T. KOKUBO and T. NAKAMURA, *Journal of the ceramic Society of Japan* **105**, 111-116 (1997).
13 H. M. Kim, F. Miyaji, T. Kokubo and T. Nakamura, *Journal of Biomedical Materials Research Part A* **32**, 409-417 (1996).
14 E. Conforto, D. Caillard, L. Mueller and F. Müller, *Acta biomaterialia* **4**, 1934-1943 (2008).
15 J. Li, G. Wang, D. Wang, Q. Wu, X. Jiang and X. Liu, *Journal of colloid and interface science* **436**, 160-170 (2014).
16 X. Lu, Y.-b. Wang, Y.-r. Liu, J.-x. Wang, S.-x. Qu, B. Feng and J. Weng, *Materials Letters* **61**, 3970-3973 (2007).
17 S. Rastegari and E. Salahinejad, *Carbohydrate Polymers* **205**, 302–311 (2019).
18 N. Namvar, E. Salahinejad, A. Saberi, M. J. Baghjeghaz, L. Tayebi and D. Vashaee, *Ceramics International* **43**, 13781-13785 (2017).
19 N. Esmati, T. Khodaei, E. Salahinejad and E. Sharifi, *Ceramics International* **44**, 17506-17513 (2018).
20 H. Rahmani and E. Salahinejad, *Ceramics International* **44**, 19200-19206 (2018).
21 M. J. Baghjeghaz and E. Salahinejad, *Ceramics International* **43**, 4680-4686 (2017).
22 E. Salahinejad and R. Vahedifard, *Materials & Design* **123**, 120-127 (2017).
23 S.-H. Jun, E.-J. Lee, S.-W. Yook, H.-E. Kim, H.-W. Kim and Y.-H. Koh, *Acta biomaterialia* **6**, 302-307 (2010).
24 R. A. Ahmed, A. M. Fekry and R. Farghali, *Applied Surface Science* **285**, 309-316 (2013).
25 L. Zhao, Y. Hu, D. Xu and K. Cai, *Colloids and Surfaces B: Biointerfaces* **119**, 115-125 (2014).
26 S. K. Mishra, J. Ferreira and S. Kannan, *Carbohydrate polymers* **121**, 37-48 (2015).
27 T. Jiang, Z. Zhang, Y. Zhou, Y. Liu, Z. Wang, H. Tong, X. Shen and Y. Wang, *Biomacromolecules* **11**, 1254-1260 (2010).
28 M. Shahrouzifar and E. Salahinejad, *Ceramics International* **45**, 10176–10181 (2019).
29 R. Vahedifard and E. Salahinejad, *Ceramics International* **43**, 8502-8508 (2017).
30 E. Salahinejad and M. J. Baghjeghaz, *Ceramics International* **43**, 10299-10306 (2017).
31 M. Shahrouzifar, E. Salahinejad and E. Sharifi, *Materials Science and Engineering: C*, 109752 (2019).
32 D. Zhitomirsky, J. Roether, A. Boccaccini and I. Zhitomirsky, *Journal of Materials Processing Technology* **209**, 1853-1860 (2009).
33 S. Karimi, E. Salahinejad, E. Sharifi, A. Nourian and L. Tayebi, *Carbohydrate polymers* **202**, 600-610 (2018).
34 D. Jugowiec, A. Łukaszczyk, Ł. Cieniek, M. Kot, K. Reczyńska, K. Cholewa-Kowalska, E. Pamuła and T. Moskalewicz, *Surface and Coatings Technology* **319**, 33-46 (2017).
35 M. Mehdipour and A. Afshar, *Ceramics international* **38**, 471-476 (2012).

This is the accepted manuscript (postprint) of the following article:
S. Rastegari, E. Salahinejad, *Morphological Optimization of Chemical-Conversion Sodium Titanate and Chitosan/Glass Nanocomposite Dip Coatings Deposited on a Titanium Alloy*, Metals and Materials International, 26 (2020) 188-195.
https://doi.org/10.1007/s12540-019-00315-1

36 S. Yamaguchi, H. Takadama, T. Matsushita, T. Nakamura and T. Kokubo, *Journal of the Ceramic Society of Japan* **117**, 1126-1130 (2009).
37 T. Kokubo and S. Yamaguchi, *Advanced Engineering Materials* **12**2010).
38 T. Kokubo and S. Yamaguchi, *Materials* **3**, 48-63 (2009).
39 S. Nishiguchi, T. Nakamura, M. Kobayashi, H.-M. Kim, F. Miyaji and T. Kokubo, *Biomaterials* **20**, 491-500 (1999).
40 L. Jonášová, F. A. Müller, A. Helebrant, J. Strnad and P. Greil, *Biomaterials* **25**, 1187-1194 (2004).
41 T. Kokubo, F. Miyaji, H. M. Kim and T. Nakamura, *Journal of the American Ceramic Society* **79**, 1127-1129 (1996).
42 S. Nishiguchi, S. Fujibayashi, H. M. Kim, T. Kokubo and T. Nakamura, *Journal of Biomedical Materials Research Part A: An Official Journal of The Society for Biomaterials, The Japanese Society for Biomaterials, and The Australian Society for Biomaterials and the Korean Society for Biomaterials* **67**, 26-35 (2003).

This is the accepted manuscript (postprint) of the following article:
S. Rastegari, E. Salahinejad, *Morphological Optimization of Chemical-Conversion Sodium Titanate and Chitosan/Glass Nanocomposite Dip Coatings Deposited on a Titanium Alloy*, Metals and Materials International, 26 (2020) 188-195.
https://doi.org/10.1007/s12540-019-00315-1

Figures

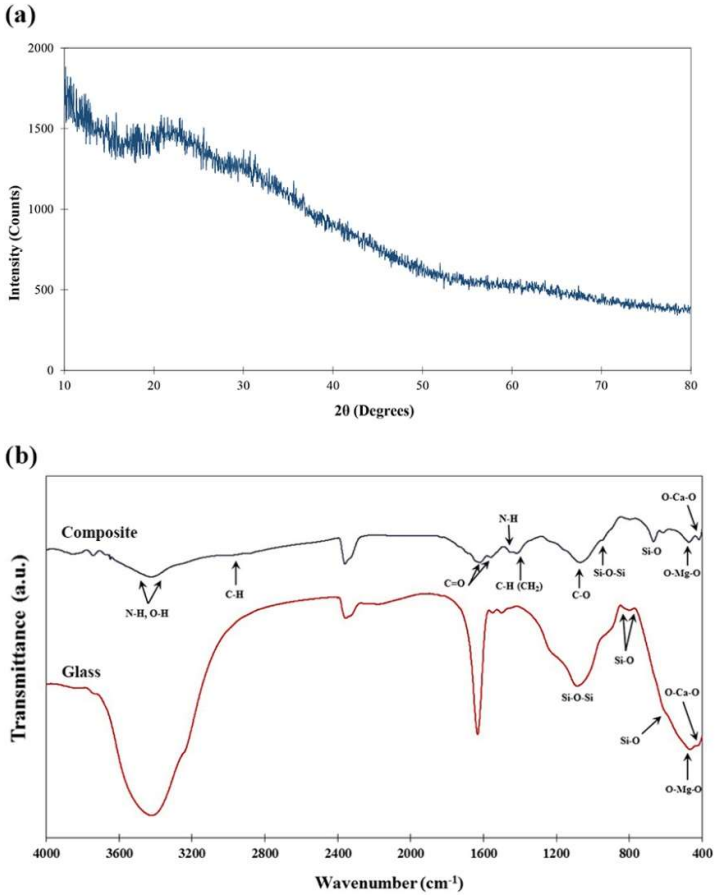

Fig. 1. XRD pattern of the synthesized silicate glass powder (a) and FTIR spectrum of the glass and composite powders (b).

This is the accepted manuscript (postprint) of the following article:
S. Rastegari, E. Salahinejad, *Morphological Optimization of Chemical-Conversion Sodium Titanate and Chitosan/Glass Nanocomposite Dip Coatings Deposited on a Titanium Alloy*, Metals and Materials International, 26 (2020) 188-195.
https://doi.org/10.1007/s12540-019-00315-1

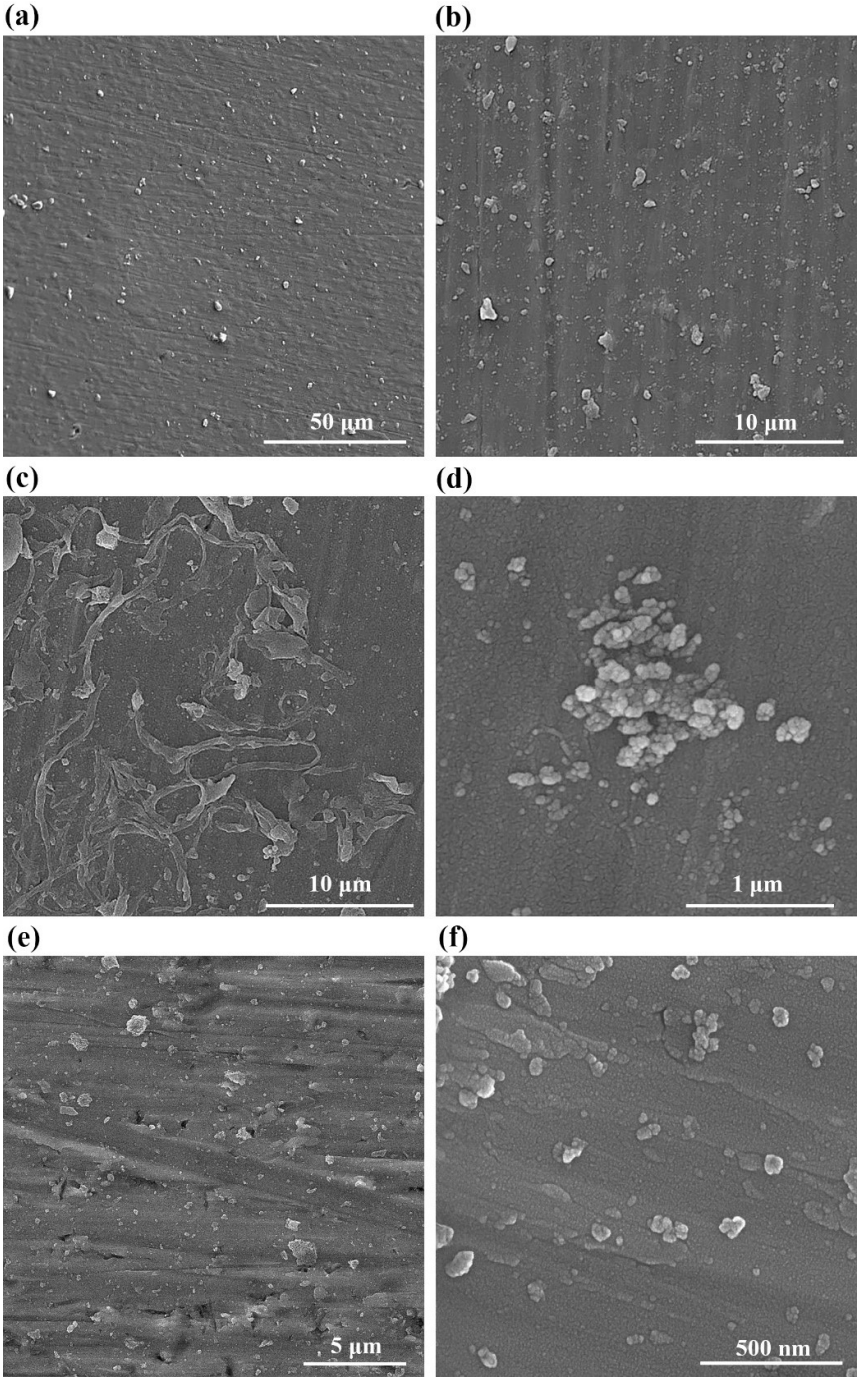

Fig. 2. Surface FESEM micrographs of the mono-layered coating with the immersion time of 30 sec (a), the mono-layered coating with the immersion time of 5 min (b, c, d) and the triple-layered coating with the immersion time of 3 min (e, f).

This is the accepted manuscript (postprint) of the following article:
S. Rastegari, E. Salahinejad, *Morphological Optimization of Chemical-Conversion Sodium Titanate and Chitosan/Glass Nanocomposite Dip Coatings Deposited on a Titanium Alloy*, Metals and Materials International, 26 (2020) 188-195.
https://doi.org/10.1007/s12540-019-00315-1

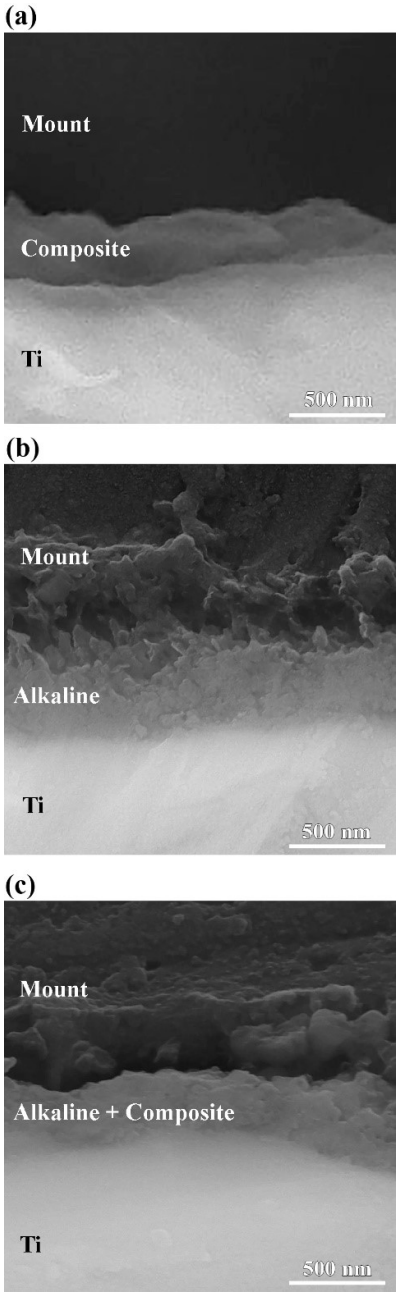

Fig. 3. Cross-sectional FESEM micrographs of the samples processed with: the triple-layered coating with the immersion time of 3 min (a), alkaline treatment (b), and alkaline + coating treatments (c). Note that the top part of each micrograph is the epoxy mount, the bottom part is the substrate and the middle part is the coatings.

This is the accepted manuscript (postprint) of the following article:
S. Rastegari, E. Salahinejad, *Morphological Optimization of Chemical-Conversion Sodium Titanate and Chitosan/Glass Nanocomposite Dip Coatings Deposited on a Titanium Alloy*, Metals and Materials International, 26 (2020) 188-195.
https://doi.org/10.1007/s12540-019-00315-1

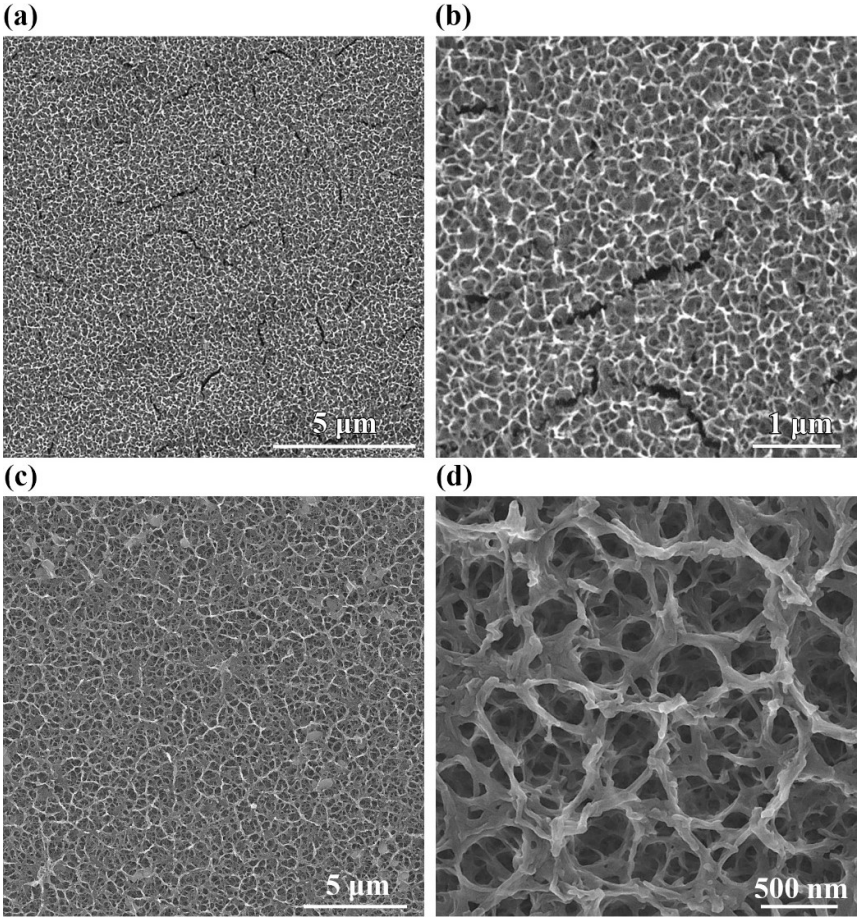

Fig. 4. Surface FESEM micrographs of the alkaline-treated samples after drying at room temperature (a and b) and 60 °C (c and d).

This is the accepted manuscript (postprint) of the following article:
S. Rastegari, E. Salahinejad, *Morphological Optimization of Chemical-Conversion Sodium Titanate and Chitosan/Glass Nanocomposite Dip Coatings Deposited on a Titanium Alloy*, Metals and Materials International, 26 (2020) 188-195.
https://doi.org/10.1007/s12540-019-00315-1

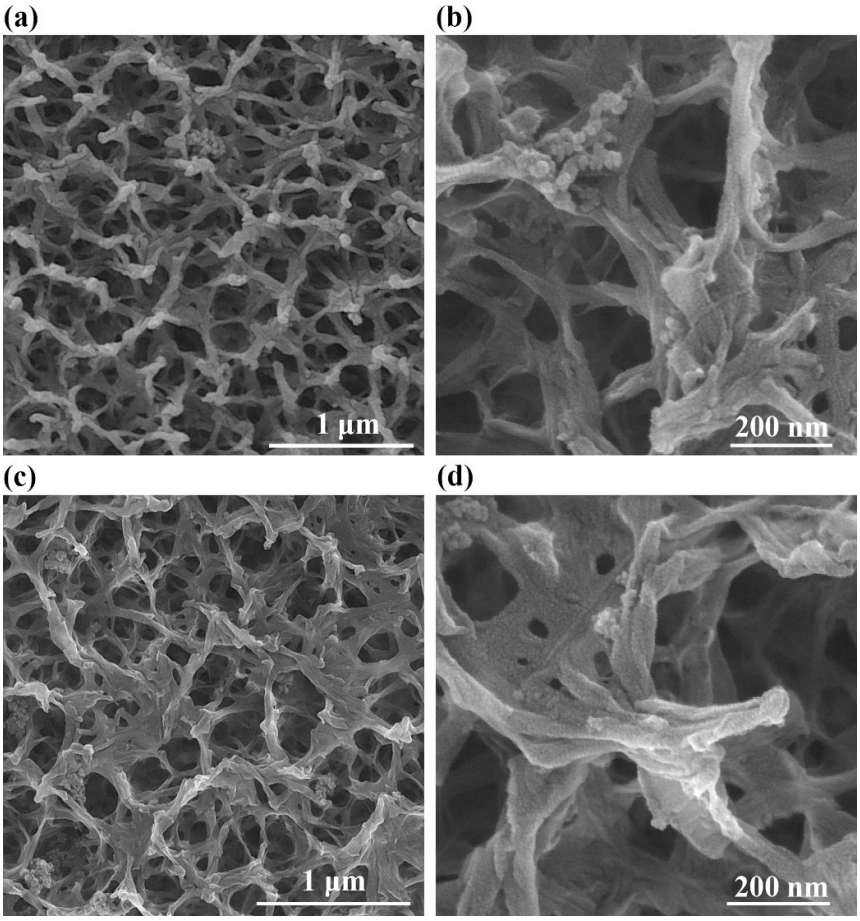

Fig. 5. Surface FESEM micrographs of the alkaline-treated samples after coating of a mono-layer with the immersion time of 5 min (a, b) and a triple layer with the immersion time of 3 min (c, d).